Materials Today: Proceedings xxx (xxxx) xxx

Contents lists available at ScienceDirect

Materials Today: Proceedings

journal homepage: www.elsevier.com/locate/matpr

Material and design parameters optimization to enhance the life of Anti-Roll bar of commercial truck

T. Vinod Kumar [a,*], M. Chandrasekaran [a], S. Padmanabhan [b], R. Saravanan [c], S. Arunkumar [a]

[a] Department of Mechanical Engineering, Vels Institute of Science, Technology and Advanced Studies (VISTAS), Chennai, Tamilnadu, India
[b] Department of Automobile Engineering, Vel Tech Rangarajan Dr. Sagunthala R & D Institute of Science and Technolgy, Chennai, India
[c] Department of Mechanical Engineering, Ellenki College of Engineering and Technology, Hyderabad, India

ARTICLE INFO

Article history:
Received 19 June 2020
Accepted 28 June 2020
Available online xxxx

Keywords:
Anti-roll bar
Front axle
Multi-body dynamics
Trial and error method
Geometric parameters

ABSTRACT

In this study, an anti-roll bar that will be used in the front axle suspension of a 25 metric tonnes capacity rigid as well as construction Trucks s focused. It is redesigned to minimize the stress concentration at the corner bends. In order to execute this, regions that are under stress concentration during the roll motion of the vehicle body are determined by using finite element analysis. Geometric parameters which constitute the form of these regions are assigned. In the light of the results obtained from the stress analyses that were carried out for the different values of these parameters, stress and mass alteration are assessed by using Trial and Error Method. The effects of these modifications on stress concentration and anti-roll bar mass are studied. Response surfaces for maximum von Mises stress and the mass of the anti-roll bar are also constructed by Multi-body Dynamics and Hyper works commercial finite element software Package. By using these results, transition from among the design candidates that gives Minimum stress concentration is determined. Four kinds of modification in design considered which includes the change of material, radius of curvature and length of the bar. The dynamic analysis based results evaluated and suggested the outperformed design.
© 2020 Elsevier Ltd. All rights reserved.
Selection and peer-review under responsibility of the scientific committee of the International Conference on Newer Trends and Innovation in Mechanical Engineering: Materials Science.

1. Introduction

During the vehicle service life, dynamic forces produce dynamic stresses which May cause fatigue failure of an anti-roll bar that is one of the basic parts of a suspension system used to reduce the roll tendency of the vehicle body. Recent studies showed that satisfying the static strength conditions does not mean that the mechanical part has infinite fatigue life Because of this, during the design process of a mechanical element, it is vital to take the fatigue life assessment into account. As long as the material and/or the manufacturing process have not been changed, tensile strength and therefore fatigue strength of a mechanical part cannot be altered. Reducing stress Concentration at the critical regions of a mechanical element is an effective alternative way to obtain a longer fatigue life. On the other hand, one of the main targets to be reached in the design of vehicle suspension components is to keep un-sprung as small as possible with a homogenous stress distribution on the part body.

Therefore an optimal design process of the mechanical part is inevitable. The typical position of ARB depicted in the Fig. 1. The role of Anti roll bar is to enhance the stability in the heavy vehicles [1-3] that is The ARB prevents the vehicle from roll due to over road irregularities, load and over speed at cornering. The rollover of Vehicle is a serious social issue which leads to loss of lives and its consequences in environment and financial aspects too [4,5]. In the heavy vehicles, the ARB system offers control at the same time it consumes energy additionally for actuators [6,7]. Also agree that the heavy vehicles controls on rolling of it, can be enhanced by ARB at uneven roads and on cornering [8]. Proposed H∞ controller and optimized the ARB system by genetic algorithm and simulation on TruckSim® software [9-11]. Improved H∞ control concepts with Linear Parameter Varying controller called passive control [12-14]. Formulated a Multi-Criteria Optimization (MCO) problem to focus the control and consumption of energy simultaneously and optimized by using genetic algorithm [15]. Improves H∞ con-

* Corresponding author.
E-mail address: vinodkmrmech@gmail.com (T. Vinod Kumar).

https://doi.org/10.1016/j.matpr.2020.06.561
2214-7853/© 2020 Elsevier Ltd. All rights reserved.
Selection and peer-review under responsibility of the scientific committee of the International Conference on Newer Trends and Innovation in Mechanical Engineering: Materials Science.

Please cite this article as: T. Vinod Kumar, M. Chandrasekaran, S. Padmanabhan et al., Material and design parameters optimization to enhance the life of Anti-Roll bar of commercial truck, Materials Today: Proceedings, https://doi.org/10.1016/j.matpr.2020.06.561

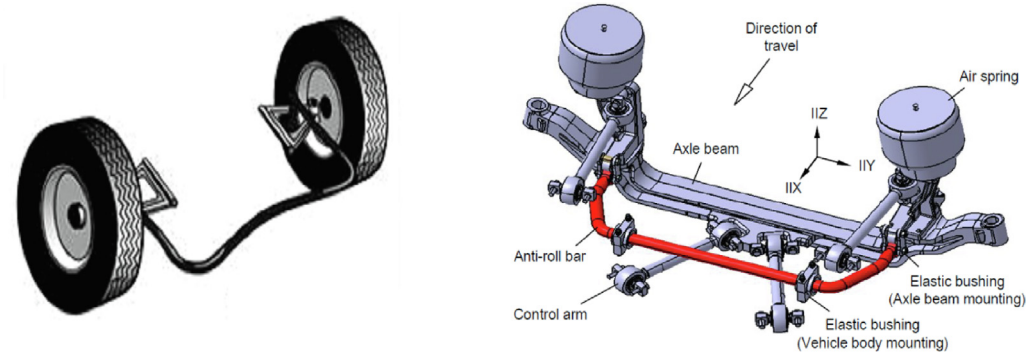

Fig. 1. Location of Anti Roll Bar in vehicle.

trols with the yaw-roll model called H∞ active (front and rear) anti-roll bars [16-19]. Improved further the design of ARB bu means of linear quadratic regulator on the system [20]. Suggested composite materials of E-Glass epoxy and HM-Carbon epoxy to increase the stiffness. In before fracture based research reported with the aspect of failure mode analysis in terms of material composition, micro structural investigation of failure bar [17,21-23]. Focused to enhance the rolling control by adopting active roll control system, continuous damping control and electronic stability control [24-26]. Investigated the influence of rubber bushing on ARB in stress distribution and fatigue behavior and reported that fatigue life improved by 21%. This research focused on failure analysis and improving its performance to serve with better stiffness at long time by alternate material and design included the changes.

2. Materials and methods

In 25 metric Tonner Construction and rigid vehicle were running with the Imported anti roll bar (ARB) imported type. The customers reported about ARB failures in such commercial vehicle

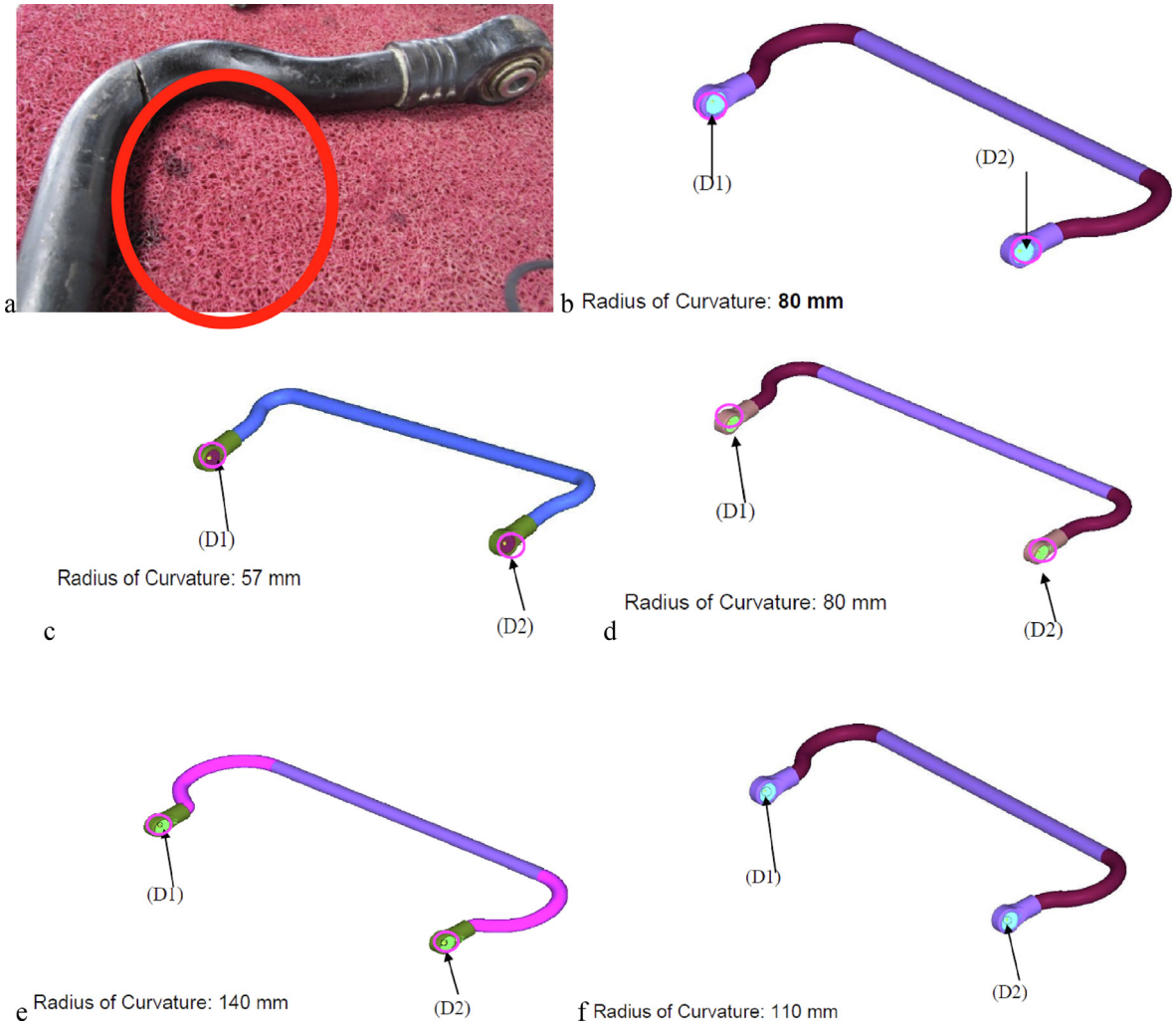

Fig. 2. Anti-Roll bar Failure in the curved portion.

Please cite this article as: T. Vinod Kumar, M. Chandrasekaran, S. Padmanabhan et al., Material and design parameters optimization to enhance the life of Anti-Roll bar of commercial truck, Materials Today: Proceedings, https://doi.org/10.1016/j.matpr.2020.06.561

Table 1
Difference between Current and Proposed Design.

	Parameters	Current Design	Proposed Designs				Unit
		Imported	Local Design 1	Local Design 2	Local Design 3	Local Design 4	
	Diameter	40	40	40	40	40	mm
	Arm Length	325	290	325	325	345	mm
	Radius of Curvature	80	57	80	100	110	mm
	Track	920	990	990	900	990	mm
	Force	26365.8	33847.4	20945.1	13479.5	17561.5	N
	Displacement	100					mm
Performance	Stiffness	263.7	338.5	209.5	134.8	175.5	N/mm
Performance	% Stiffness Diff	0%	28%	-21%	-49%	-33%	
Performance	Roll Stiffness (spring+arb+tire)	5607	6167	5267	4471	4936	Nm/deg
Performance	% Roll Stiffness Diff	0%	10%	-6%	-21%	-12%	
Durability	Yield Limit	1180			900		N/mm^2
Durability	Stress	1481	1700	1333	900.5	1037	N/mm^2
Durability	% Stress Above Yield	26%	89%	48%	0%	15%	
						-12%	

Compared to imported yield 1180 MPa

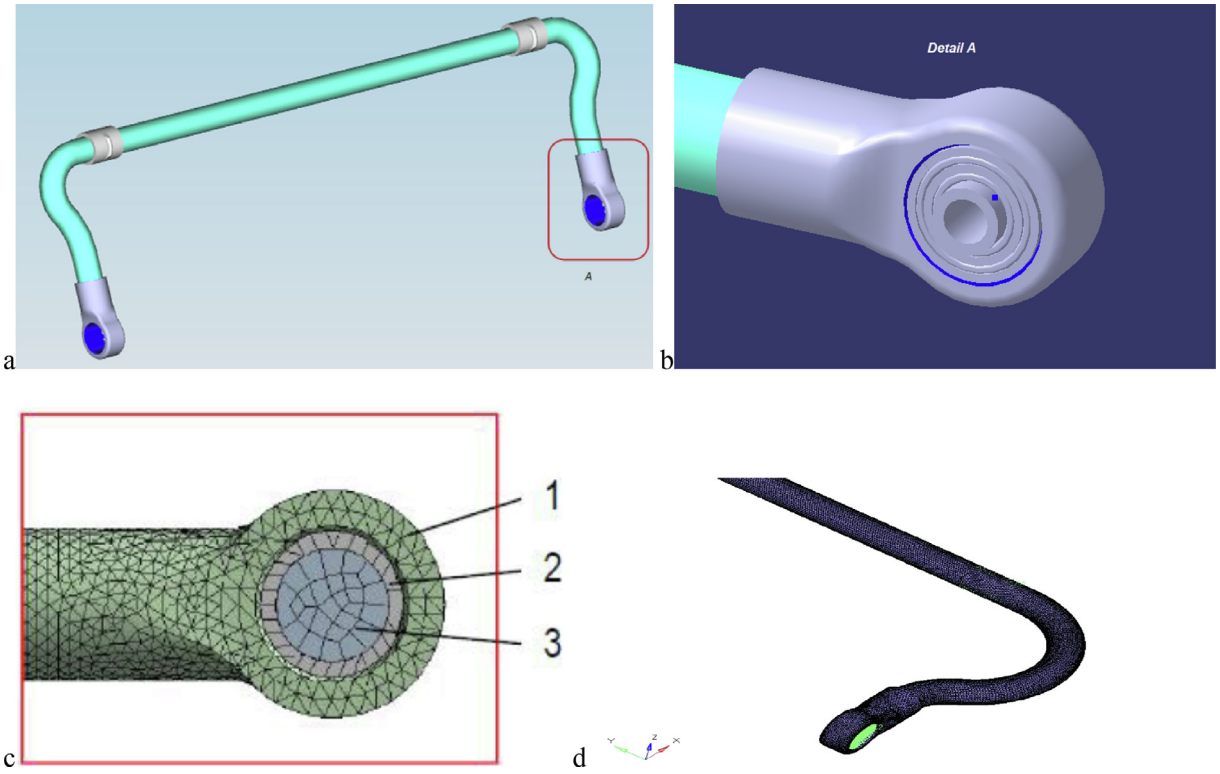

Fig. 3. The Figure 3a shows the CAD model of anti-roll bar, the Figure 3b depicts the detail of Bushing at section A in the Figure 3a. the Figure 3c shows the meshed details at bearing in which the 1 indicates Anti-roll bar, 2 denotes Elastic bushing and 3 marked for showing connection bolt. The Figure 3d shows the meshed model of ARB.

that after 30,000 Km the anti roll bar failure by broken at near the curvature as shown in the Fig. 2a.

2.1. Root cause analysis

By Using CAE tool, field failure of antiroll bar was re modeled for analyzing the root cause of the failure. In the correlation wit was found that the stress concentration is more in the curved portion. Based on the design constraint, antiroll bar was redesigned for reduced Stress concentration at the curved portion by optimizing the shape of critical region.

2.2. Proposed ARB

The conventional ARB made up of 55CR3 material. It is suggested that if we raise the yield strength with to 50CrV4 to avoid

Please cite this article as: T. Vinod Kumar, M. Chandrasekaran, S. Padmanabhan et al., Material and design parameters optimization to enhance the life of Anti-Roll bar of commercial truck, Materials Today: Proceedings, https://doi.org/10.1016/j.matpr.2020.06.561

the failure, because the alternate material which suggested remains unaltered properties other than little higher yield strength (refer Table 1). Hence 50CrV4 material was adopted for investigation of proposed designs. The suggestion was alter the radius of curvature either increase or decrease. If the change radius of curvature demands little alteration in arm length of ARB and the same is unavoidable. Hence change of material and radius of curvature are focused in the proposed designs. The conventional and proposed designs of ARB are as follows:

2.3. About the models

The hyper works 11.O used for meshing the CAD Model and FEM software of Radioss employed for stress analysis. The more number of Iteration reduced the time consumption for solving problem. This study initially performed in first order. After comparison of stress for all the iteration and found the solution later for more accurate result, the second order (Batch mode) preferred. The meshing criteria were Tetra 4 – 1st order (301153 elements > 65863 Nodes) for basic analysis and Tetra 10 – 2nd order (301153 elements < 462018 nodes involved) for final analysis but ultimate results considered from the 2nd order model. Maximum element length was 11.5 mm and Minimum element length was 0.3 mm Fig. 3.

2.4. Simulation criteria

Two cases considered for CAE calculation the first one was Jounce and Rebound as 100 mm in upward and downward direction of wheel centers and this simulation is determine if there is any linkage lockup in these extreme condition. The other was Axle Roll, 5.1 deg (standard criteria construction application vehicle)

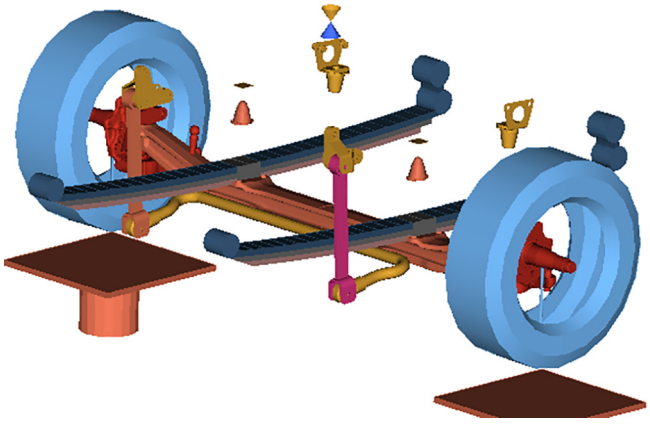

Fig. 4. Multi-body dynamics Model of Anti Roll Bar.

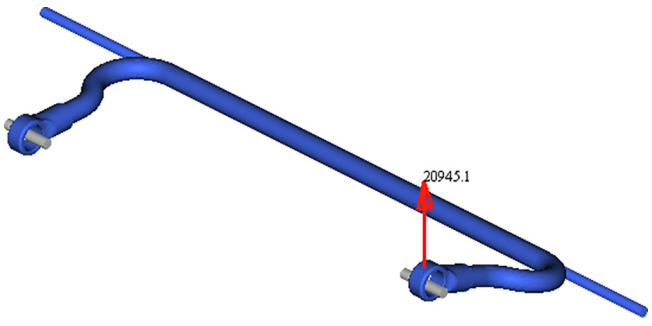

Fig. 5. Load conditions.

= 100 mm in upward and downward direction of wheel centers) and the Max axle Roll possible for this front suspension = 11.0 deg (200 mm in upward and downward direction of wheel centers). The CAE tools employed for simulation correlation and design analysis are: Motion View and Motion Solve (force and displacement calculation), Hyper-mesh (antiroll bar meshing - preprocessing), 'optistruct' (FE Solver - Linear) and Hyper-view (post processing).

3. Simulation methods in Multi-Body Dynamics

The displacement details are obtained by using multi-body Dynamic. To do this activity the model has been created in the multi-body dynamics by using Hyper works Motion Viewer. And all the design Iteration has to be carried out with design constraints Figs. 4–6.

3.1. Design analysis process

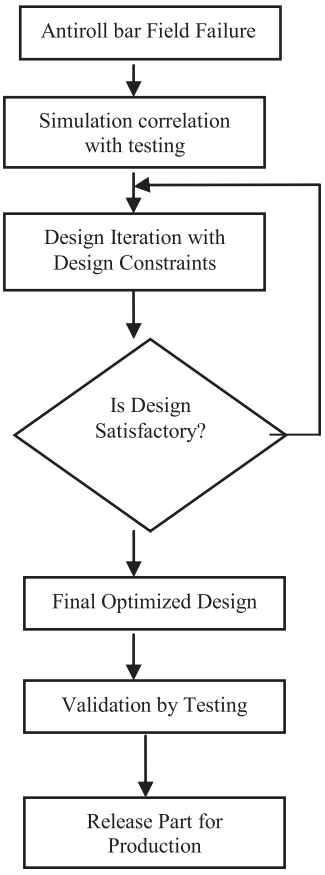

4. Results and discussion

The maximum Von mises stress, σ_{max} values for various design iteration has been calculated for anti roll bar. The design constraints specified by the trial and error methods. The test was carried out for calculating the effects of torsion. The maximum Von Misses stress considered.

4.1. Analysis on imported design of ARB model

In the Imported design the values as it is considered for modeling. ARB diameter of 40 mm, according to the design profile its arm length is 325 mm. The track as per specification of ARB, was 920 mm. The Stress Plot of Imported Design Torsion Bar (ARB) with

Please cite this article as: T. Vinod Kumar, M. Chandrasekaran, S. Padmanabhan et al., Material and design parameters optimization to enhance the life of Anti-Roll bar of commercial truck, Materials Today: Proceedings, https://doi.org/10.1016/j.matpr.2020.06.561

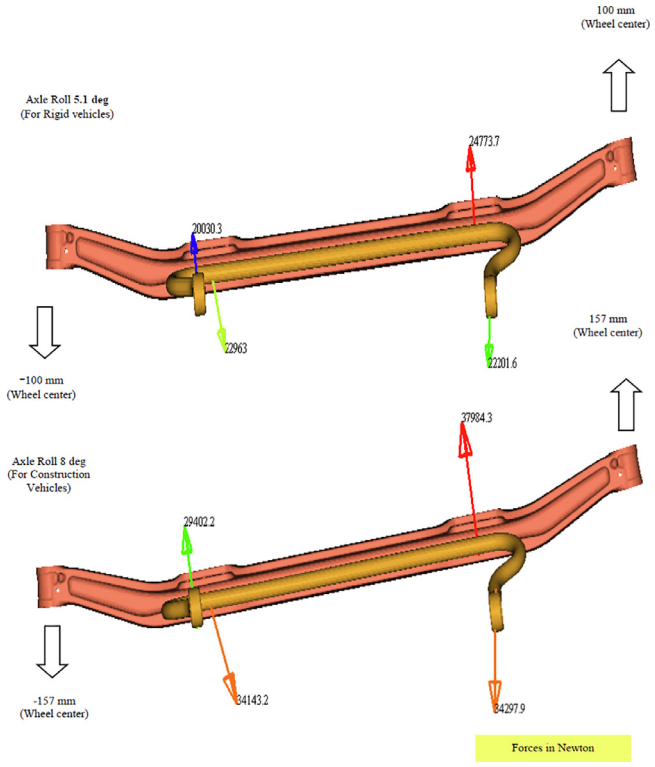

Fig. 6. Force Comparison of Anti-Roll bar.

radius of curvature 80 mm is depicted in the Fig. 7a. The material of the ARB is 55Cr3 (EN 10089) and its yield Strength is 1180 MPa. The maximum allowable displacements under the axial roll load condition which applied at ARB and drop link joint. The displacements in direction wise at left as well as right end furnished below the stress plot. The force obtained for 100 mm displacement of ARB was 26356.8 N. The stiffness was estimated that 263.7 N mm. the roll stiffness due to the cumulative effects of ARB, tire and spring systems that 5607Nm per degree of turn. The yield limit as specified was 1180 N per square mm. but the stress induced was found that 1481 N per square mm and it is 26% excess than the yield strength of the material 55Cr3. As this existing ARB model is used as bench mark for measuring performance of three proposed design of ARB. The percentage of stiffness difference and roll stiffness difference as zero with respect to it.

4.2. Analysis on proposed Design-1of ARB model

In the proposed design with lesser radius of curvature (Local Design 1), the value ARB diameter 40 mm considered as it was. Due to change of radius of curvature (Reduction to 57 mm from 80 mm) in the design profile of imported ARB, the tract was 990 mm. its arm length is 290 mm. The Fig. 7b depicts the Stress Plot of proposed Design of Torsion Bar (ARB) with radius of curvature 57 mm (proposed design 1). The material of the ARB is 50CrV4 (steel (EN 10089) and its yield strength 900 MPa. The maximum allowable displacements under the axial roll load condition which applied at ARB and drop link joint is fixed as 100 mm. The displacements in direction wise at left as well as right end furnished below the stress plot. . The force obtained for 100 mm displacement of ARB was 33847.4 N. The stiffness was estimated that 338.5 N mm and it is 28% higher than the imported design ARB. The roll stiffness which due to the cumulative effects of ARB, tire and spring systems that 6167 Nm per degree of turn and it is 10% higher than that of imported design ARB. The yield limit as specified was 900 N per square mm. But the stress induced was found that 1700 N per square mm. it is 89% higher than that of the yield strength of material 50CrV4 steel (EN 10089).

4.3. Analysis on proposed Design-2 of ARB model

In the proposed design with equal radius of curvature (Local Design 2) as like as imported model but change of material of the component is 50CrV4 steel (EN 10089), the value ARB diameter 40 mm considered as it was. As there were no changes in radius of curvature (80 mm) in the design profile of imported ARB arm length is 290 mm. The tract considered for this case as like as local design 1 as 990 mm. its. The Fig. 7c depicts the Stress Plot of proposed Design of Torsion Bar (ARB) with radius of curvature 80 mm (proposed design 2). The material of the ARB is 50CrV4 steel (EN 10089) and its yield strength 900 MPa. The maximum allowable displacements under the axial roll load condition which applied at ARB and drop link joint is fixed as 100 mm. The displacements in direction wise at left as well as right end furnished below the stress plot. The force obtained for 100 mm displacement of ARB was 20945.1 N. The stiffness was estimated that 209.5 N mm and it is 21% lesser than the imported design ARB. The roll stiffness which due to the cumulative effects of ARB, tire and spring systems that 5267 Nm per degree of turn and it is 6% lesser than that of imported design ARB. The yield limit as specified was 900 N per square mm. But the stress induced was found that 1333 N per square mm. it is 48% higher than that of the yield strength of material 50CrV4 steel (EN 10089).

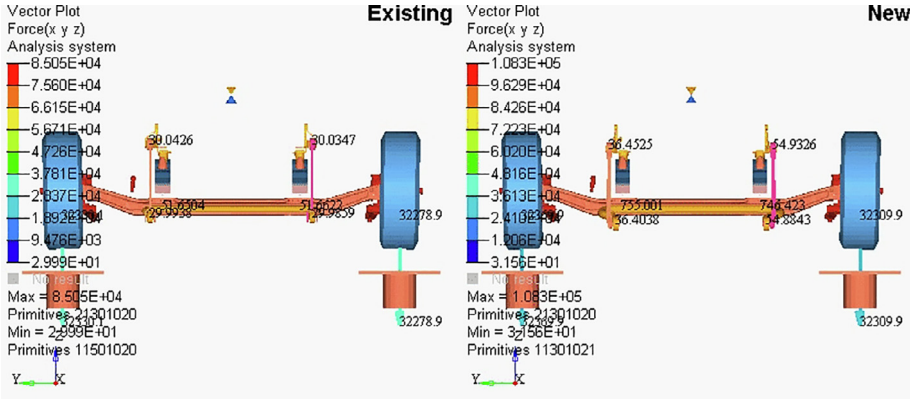

Fig. 7. Displacements – Multi-body Dynamics.

Please cite this article as: T. Vinod Kumar, M. Chandrasekaran, S. Padmanabhan et al., Material and design parameters optimization to enhance the life of Anti-Roll bar of commercial truck, Materials Today: Proceedings, https://doi.org/10.1016/j.matpr.2020.06.561

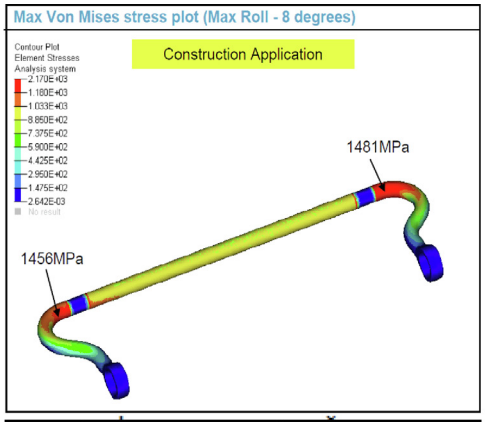

units - mm	LH (D2)			RH (D1)		
	X	Y	Z	X	Y	Z
8 deg	16.213	-13.7281	-58.6505	-20.205	-3.846	74.2676

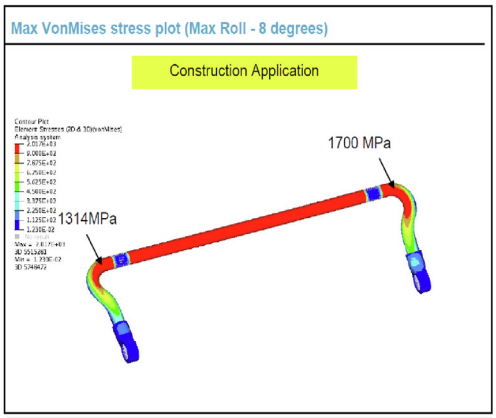

	LH			RH		
	X	Y	Z	X	Y	Z
8 deg	9.566	-11.305	-52.6851	-12.035	-0.4254	67.1482

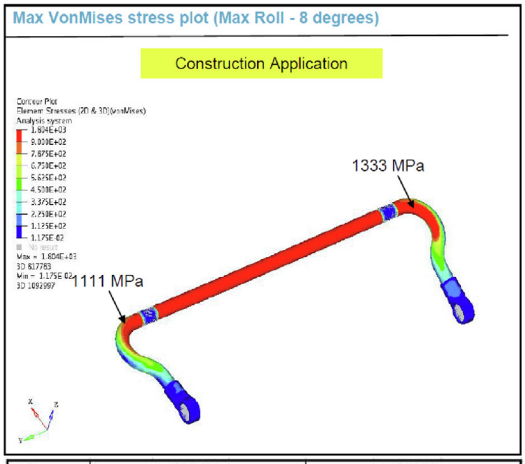

units - mm	LH (D2)			RH (D1)		
	X	Y	Z	X	Y	Z
8 deg	8.641	-11.7592	-54.16	-10.841	0.2258	68.5552

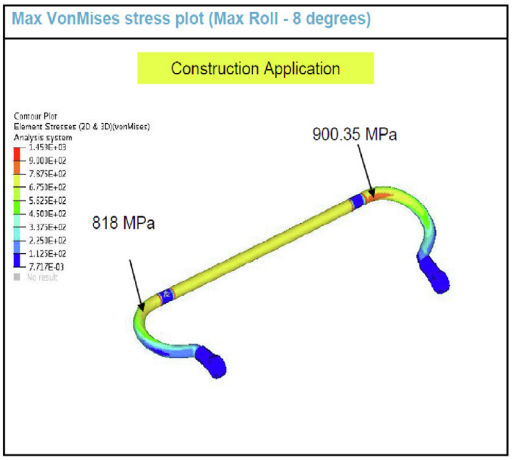

units - mm	LH (D2)			RH (D1)		
	X	Y	Z	X	Y	Z
8 deg	8.641	-11.7592	-54.16	-10.841	0.2258	68.5552

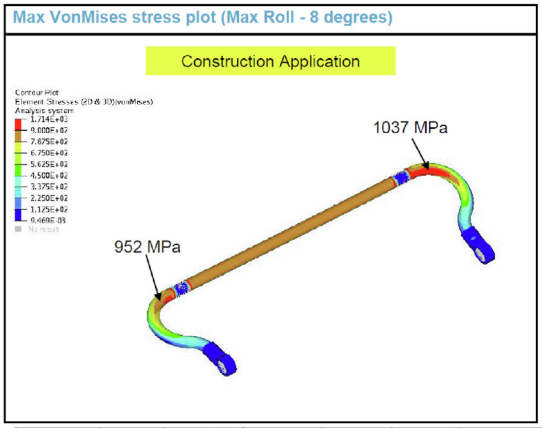

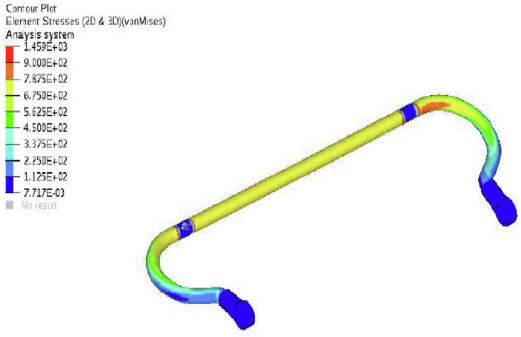

units - mm	LH (D2)			RH (D1)		
	X	Y	Z	X	Y	Z
8 deg	8.641	-11.7592	-54.16	-10.841	0.2258	68.5552

Fig. 8. Von Mises Stress analysis Plot Minimized stress at the critical region.

4.4. Analysis on proposed Design-3 of ARB model

In the proposed design with higher radius of curvature (Local Design 3) than the imported model and change of material of the component, the value ARB diameter 40 mm considered as it was. As there is increase of radius of curvature (from 80 mm to 140 mm) in the design profile of imported ARB arm length revised to 385 mm. The tract considered for this case as like as local design

Please cite this article as: T. Vinod Kumar, M. Chandrasekaran, S. Padmanabhan et al., Material and design parameters optimization to enhance the life of Anti-Roll bar of commercial truck, Materials Today: Proceedings, https://doi.org/10.1016/j.matpr.2020.06.561

1 and 2 as 990 mm. The Fig. 7d depicts the Stress Plot of proposed Design of Torsion Bar (ARB) with radius of curvature 140 mm (proposed design 2). The material of the ARB is 50CrV4 steel (EN 10089) and its yield strength 900 MPa. The maximum allowable displacements under the axial roll load condition which applied at ARB and drop link joint is fixed as 100 mm. The displacements in direction wise at left as well as right end furnished below the stress plot. The force obtained for 100 mm displacement of ARB was 13479.5 N. The stiffness was estimated that 134.8 N mm and it is 49% lesser than the imported design ARB. The roll stiffness which due to the cumulative effects of ARB, tire and spring systems that 4451Nm per degree of turn and it is 21% lesser than that of imported design ARB. The yield limit as specified was 900 N per square mm. But the stress induced was found that 900.35 N per square mm. it is nearly equal to the yield strength of material 50CrV4 steel (EN 10089) and also 23.699% less than the conventional tortional bar.

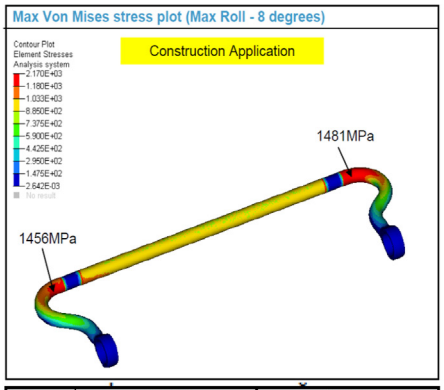

a

units - mm	LH (D2)			RH (D1)		
8 deg	X	Y	Z	X	Y	Z
	16.213	-13.7281	-58.6505	-20.205	-3.846	74.2676

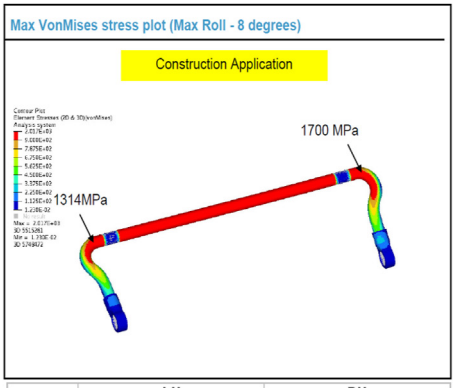

b

	LH			RH		
8 deg	X	Y	Z	X	Y	Z
	9.566	-11.305	-52.6851	-12.035	-0.4254	67.1482

4.5. Analysis on proposed Design-3 of ARB model

In the proposed design with higher radius of curvature (Local Design 4) than the imported model and change of material of the component, the value ARB diameter 40 mm considered as it was. As there is increase of radius of curvature (from 80 mm to 110 mm) in the design profile of imported ARB arm length revised to 345 mm. The tract considered for this case as like as local design 1 and 2 as 990 mm. The Fig. 7d depicts the Stress Plot of proposed Design of Torsion Bar (ARB) with radius of curvature 110 mm (proposed design 2). The material of the ARB is 50CrV4 steel (EN 10089) and its yield strength 900 MPa. The maximum allowable displacements under the axial roll load condition which applied at ARB and drop link joint is fixed as 100 mm. The displacements in direction wise at left as well as right end furnished below the stress plot. The force obtained for 100 mm displacement of ARB was 17561.6 N. The stiffness was estimated that 175.6 N mm and it is 33% lesser than the imported design ARB. The roll stiffness which due to the cumulative effects of the ARB, tire and spring systems that 4936Nm per degree of turn and it is 13% lesser than that of imported design ARB. The yield limit as specified was 900 N per square mm. But the stress induced was found that 1037 N per square mm. it is 15% higher than the yield strength of material 50CrV4 steel (EN 10089) and also 12.11% less than the conventional tortional bar (Fig. 8).

5. Conclusion

This project was conducted to eliminate the field failure of the Imported Anti-roll bar for which we have developed a local design with low cost by in-house facility. And the design iteration is carried out by optimizing the Radius of curvature of the curved portion and the arm length of Anti-roll bar to reduce the stress concentration prevailing in the existing design. In each local design proposals had its unique pros and cons and were verified and validated during durability test and the performance was compared to ascertain the optimum design. All 4 design proposals and reports were consolidated and the analysis reports were verified. In the comparison list we have selected the local Design 3 and local design 4 for further investigation. By comparing the local Design 3 & 4, we found that the percentage of the roll stiffness is high in case of local design 3 as compared to local design 4 are 21% and 12% lesser than yield value respectively. The stress also observed in local design 4 is also within the limit. In this design and analysis study of Anti-Roll bar, the solution arrived through design Iteration method with existing in house resources. And Overall cost saving achieved is of 20% with this localized part design solution. The material change gives only 22% reduction on yield stress of material in stress but cumulatively with design changes 0% to 15% than yield stress of the material.

Declaration of Competing Interest

The authors declare that they have no known competing financial interests or personal relationships that could have appeared to influence the work reported in this paper.

References

[1] V.T. Vu, O. Sename, L. Dugard, P. Gaspar, Active anti-roll bar control using electronic servo valve hydraulic damper on single unit heavy vehicle, IFAC-PapersOnLine 49 (11) (2016) 418–425, https://doi.org/10.1016/j.ifacol.2016.08.062.

[2] V.T. Vu, P. Gaspar, Performance and robustness assessment of H∞ active anti-roll bar control system by using a software environment, IFAC-PapersOnLine 52 (5) (2019) 255–260, https://doi.org/10.1016/j.ifacol.2019.09.041.

[3] V.-T. Vu, O. Sename, L. Dugard, P. Gaspar, Multi objective H∞ active anti-roll bar control for heavy vehicles, IFAC-PapersOnLine 50 (1) (2017) 13802–13807, https://doi.org/10.1016/j.ifacol.2017.08.2071.

[4] V.T. Vu, O. Sename, L. Dugard, P. Gaspar, H∞/LPV controller design for an active anti-roll bar system of heavy vehicles using parameter dependent weighting functions, Heliyon 5 (6) (2019) e01827, https://doi.org/10.1016/j.heliyon.2019.e01827.

Please cite this article as: T. Vinod Kumar, M. Chandrasekaran, S. Padmanabhan et al., Material and design parameters optimization to enhance the life of Anti-Roll bar of commercial truck, Materials Today: Proceedings, https://doi.org/10.1016/j.matpr.2020.06.561

[5] H. Bayrakceken, S. Tasgetiren, K. Aslantas, Fracture of an automobile anti-roll bar, Eng. Fail. Anal. 13 (5) (2006) 732–738, https://doi.org/10.1016/j.engfailanal.2005.04.002.
[6] H. Her, K. Yi, J. Suh, C. Kim, Development of integrated control of electronic stability control, continuous damping control and active anti-roll bar for vehicle yaw stability, IFAC Proc. 46 (21) (2013) 83–88, https://doi.org/10.3182/20130904-4-JP-2042.00152.
[7] V.-T. Vu, O. Sename, L. Dugard, P. Gaspar, H∞ active anti-roll bar control to prevent rollover of heavy vehicles: a robustness analysis, IFAC-PapersOnLine 49 (9) (2016) 99–104, https://doi.org/10.1016/j.ifacol.2016.07.503.
[8] M.K. Nikhil, D.H. Daspute, Dynamic analysis of anti roll bar, Mater. Today Proc. 5 (5) (2018) 12490–12498, https://doi.org/10.1016/j.matpr.2018.02.230.
[9] M. Cerit, E. Nart, K. Genel, Investigation into effect of rubber bushing on stress distribution and fatigue behaviour of anti-roll bar, Eng. Fail. Anal. 17 (5) (2010) 1019–1027, https://doi.org/10.1016/j.engfailanal.2010.01.009.
[10] V.S. Shaisundaram, M. Chandrasekaran, S. Mohan Raj, R. Muraliraja, Investigation on the effect of thermal barrier coating at different dosing levels of cerium oxide nanoparticle fuel on diesel in a CI engine, Int. J. Ambient Energy 41 (1) (2020) 98–104.
[11] V.S. Shaisundaram, M. Chandrasekaran, M. Shanmugam, S. Padmanabhan, R. Muraliraja, L. Karikalan, Investigation of Momordica charantia seed biodiesel with cerium oxide nanoparticle on CI engine, Int. J. Ambient Energy (2019) 1–5.
[12] V.S. Shaisundaram, M. Chandrasekaran, S. Mohan Raj, R. Muraliraja, T. Vinodkumar, Control of carbon dioxide emission in automobile vehicles using CO2 scrubber, Int. J. Ambient Energy 40 (7) (2019) 699–703.
[13] V.S. Shaisundaram, L. Karikalan, M. Chandrasekaran, Experimental investigation on the effect of cerium oxide nanoparticle fuel additives on pumpkin seed oil in CI engine, Int. J. Vehicle Struct. Syst. (IJVSS) 11 (3) (2019).
[14] R. Muraliraja, J. Sudagar, R. Elansezhian, A.V. Raviprakash, R. Dhinakaran, V.S. Shaisundaram, M. Chandrasekaran, Estimation of Zwitterionic surfactant response in electroless composite coating and properties of Ni–P–CuO (Nano) coating, Arabian J. Sci. Eng. 44 (2) (2019) 821–828.
[15] R. Muraliraja, R. Elansezhian, Influence of nickel recovery efficiency on crystallinity and microhardness of electroless Ni–P coatings and optimisation using Taguchi technique, Trans. IMF 93 (3) (2015) 126–132.
[16] R. Muraliraja, D. Sendilkumar, D.R. Elansezhian. (2015). Prediction and Supplementation of Reducing Agent to Improve the Coating Efficiency and Wear Behavior of Electroless Ni-P Plating. Int. J. Electrochem. Sci., 10, 5536-47.
[17] S. Baskar, V. Vijayan, S. Saravanan, A.V. Balan, A. Godwin Antony, Effect of Al2O3, aluminium alloy and fly ash for making engine component, Int. J. Mech. Eng. Technol. (IJMET) 9 (12) (2018) 91–96.
[18] A. Godwin Antony, V. Vijayan, S. Saravanan, S. Baskar, M. Loganathan, Analysis of wear behaviour of aluminium composite with silicon carbide and titanium reinforcement, Int. J. Mech. Eng. Technol. 9 (2018) 681–691.
[19] S. Saravanan, A. Godwin Antony, V. Vijayan, M. Loganathan, S. Baskar, Synthesis of SiO2 nano particles by using sol-gel route, Int. J. Mech. Eng. Technol. 1 (2019) 785–790.
[20] S. Dinesh, A. Godwin Antony, K. Rajaguru, V. Vijayan, Experimental investigation and optimization of material removal rate and surface roughness in centerless grinding of magnesium alloy using grey relational analysis, Mech. Mech. Eng. 21 (2017) 17–28.
[21] S. Dinesh, K. Rajaguru, V. Vijayan, A. Godwin Antony, Investigation and prediction of material removal rate and surface roughness in CNC turning of EN24 alloy steel, Mechanics and Mechanical Engineering , 20(2016), pp. 451-466.
[22] B. Suresh Kumar, V. Vijayan, N. Baskar, Burr dimension analysis on various materials for convenantionally and CNC drilled holes, Mech. Mech. Eng. 20 (2016) 347–354.
[23] Baskar Sanjeevi, Karikalan Loganathan, "Synthesis of MWCNT Nanofluid by using Two Step Method", Thermal Science, International Scientific Journal, Published Online: November 2019.
[24] Jishuchandran, K. Manikandan, R. Ganesh, S. Baskar, "Effect of Nano-Material on the Performance Patterns of Waste Cooking Biodiesel Fuelled Diesel Engine" International Journal of Ambient Energy, pages 1-16.
[25] D. Arunkumar, M. Ramu, R. Murugan, S. Kannan, S. Arun, S. Baskar, Investigation of heat transfer of wall with and without using phase change material, Mater. Today Proc. (2020), https://doi.org/10.1016/j.matpr.2020.01.220.
[26] K. Logesh, S. Baskar, M. Azeemudeen, B. Praveen Reddy, G. Venkata Subba Sai Jayanth, Analysis of cascade vapour refrigeration system with various refrigerants, Mater. Today Proc. 18 (2019) 4659–4664, https://doi.org/10.1016/j.matpr.2019.07.450.

Please cite this article as: T. Vinod Kumar, M. Chandrasekaran, S. Padmanabhan et al., Material and design parameters optimization to enhance the life of Anti-Roll bar of commercial truck, Materials Today: Proceedings, https://doi.org/10.1016/j.matpr.2020.06.561